AWARD NUMBER: W81XWH-14-1-0434

TITLE: Modeling TSC and LAM Using Patient-Derived Induced Pluripotent Stem Cells

PRINCIPAL INVESTIGATOR: William L Stanford

CONTRACTING ORGANIZATION: University of Ottawa
Ottawa, ON Canada

REPORT DATE: October 2016

TYPE OF REPORT: Annual report

PREPARED FOR: U.S. Army Medical Research and Materiel Command
Fort Detrick, Maryland 21702-5012

REPORT DOCUMENTATION PAGE

Form Approved
OMB No. 0704-0188

1. REPORT DATE	2. REPORT TYPE	3. DATES COVERED
October 2016	Annual report	09/30/2015-09/29/2016

4. TITLE AND SUBTITLE

Modeling TSC and LAM Using Patient-Derived Induced Pluripotent Stem Cells

5a. CONTRACT NUMBER
W81XWH-14-1-0434

5b. GRANT NUMBER
TS130051

5c. PROGRAM ELEMENT NUMBER

6. AUTHOR(S) William Stanford (PI - site 1) & Arnold Kristof (site 2)

E-Mail: wstanford@ohri.ca;

5d. PROJECT NUMBER
0010501154-001

5e. TASK NUMBER

5f. WORK UNIT NUMBER

7. PERFORMING ORGANIZATION NAME(S) AND ADDRESS(ES)

AND ADDRESS(ES)

Site 1
University of Ottawa/OHRI
501 Smyth Rd.
Ottawa, ON Canada

Site 2
McGill University Health Centre
Royal Victoria Hospital
687 Pine Ave. W
Montreal, QC, Canada

8. PERFORMING ORGANIZATION REPORT NUMBER

9. SPONSORING / MONITORING AGENCY NAME(S) AND ADDRESS(ES)

U.S. Army Medical Research and Materiel Command
Fort Detrick, Maryland 21702-5012

10. SPONSOR/MONITOR'S ACRONYM(S)

11. SPONSOR/MONITOR'S REPORT NUMBER(S)

12. DISTRIBUTION / AVAILABILITY STATEMENT

Approved for Public Release; Distribution Unlimited

13. SUPPLEMENTARY NOTES

14. ABSTRACT

Tuberous sclerosis complex (TSC) is a multi-organ genetic disorder with an estimated incidence of one in 6,000 live births due to mutations in either TSC1 or TSC2. About 30% of women with TSC have lymphangioleiomyomatosis (LAM), a progressive lung disease characterized by abnormal proliferation of smooth muscle-like cells throughout the lungs, leading to lung destruction and eventual respiratory failure. The cause of the tumor development in various tissues is not well understood, in part due to a lack of human TSC1 or TSC2 deficient human cells to study the biology of the disease and perform drug screens. We have now made TSC2 deficient human cells using patient induced pluripotent stem cells (iPSCs), lentiviral knockdown, and CRISPR/Cas9 genome editing in embryonic stem cells (ESCs). We have characterized the iPSCs extensively and found that they display abnormal cell size, autophagy regulation, metabolic activity, hyperactive mTOR signaling, and differentiation – all characteristics of TSC and LAM cells.

15. SUBJECT TERMS

Tuberous Sclerosis Complex, Lymphangioleiomyomatosis (LAM), disease modeling

16. SECURITY CLASSIFICATION OF:			17. LIMITATION OF ABSTRACT	18. NUMBER OF PAGES	19a. NAME OF RESPONSIBLE PERSON
a. REPORT	b. ABSTRACT	c. THIS PAGE			USAMRMC
Unclassified	Unclassified	Unclassified	Unclassified	28	19b. TELEPHONE NUMBER *(include area code)*

TABLE OF CONTENTS

INTRODUCTION

Tuberous Sclerosis Complex (TSC) is a multisystem disorder causing low-grade neoplastic tumours in the brain, kidneys, heart, eyes, lung, and skin which arises from germline and subsequent second-hit somatic mutations in the *TSC1* or *TSC2* genes, most predominantly *TSC2* (reviewed in [1]). The TSC-related neoplasm leading to the greatest morbidity and mortality is Lymphangioleiomyomatosis (LAM). LAM is characterized by abnormal proliferation of smooth muscle-like cells (SMCs) in the lung, leading to destruction of the lung tissue and respiratory failure, eventually leading to death (reviewed in 2). The average age of onset of LAM symptoms is 35 years, it affects women almost exclusively, and respiratory failure generally occurs within 10-20 years of diagnosis. LAM affects at least 30% of women with TSC and accounts for the majority of LAM cases (TSC-LAM), however LAM also occurs spontaneously in women who were not born with TSC. While loss of function mutations in *TSC1* or, most frequently, *TSC2* underlie the majority, if not all, of TSC-LAM and sporadic LAM cases, the etiology of LAM is poorly understood, which has severely limited treatment options. *TSC1* and *TSC2* encode the proteins Tuberin and Hamartin, respectively. Tuberin contains a GTPase activating protein domain which inhibits the G-protein Rheb. Rheb directly interacts with and activates mTOR (reviewed in [3]). mTOR nucleates two distinct macromolecular protein complexes. mTOR complex 1 (mTORC1) is inhibited by Rapamycin, contains the protein Raptor, and controls mitogen- and nutrient-sensitive cell growth. mTORC2, which contains the protein Rictor, is resistant to Rapamycin acutely, but can be inhibited with prolonged exposure; mTORC2 controls cytokinesis and cell survival [4]. TSC2/ Tuberin integrates growth factor and metabolic signaling and modulates mTOR activity. Although Rapamycin slowed progression of disease in multicenter controlled trials, tumors were not completely eliminated, or tended to recur upon cessation of treatment [5, 6].

While all *TSC2*-deficient cells exhibit common oncogenic molecular signatures (such as increased mTOR activity), other defects are unique to specific tumour types. For example, *TSC2*-deficient brain tumour cells uniquely express markers of early neuronal differentiation, while LAM cells express estrogen and prolactin receptors. Thus, the disease phenotype of TSC2-deficient tumours can differ depending on the origin of the cells that comprise the particular tumour type. **Current cellular and animal models of TSC2-deficiency do not fully recapitulate the molecular and behavioral characteristics of TSC neurological tumors nor LAM cells**, and thus treatment options for TSC and LAM are limited. This is, in part, due to the lack of human TSC1 or TSC2 deficient cells that can be used to model TSC-related neoplasms and perform drug screens to develop novel treatments. Thus, we clearly need better cellular and animal models of TSC that reflect how the tumors are initiated, propagated, and maintained *in vivo*.

The Aims of our study are to:

1. Generate TSC2 heterozygous and homozygous human induced pluripotent stem cell (iPSC) and embryonic stem cell (ESC) lines.
2. Model TSC and LAM using in vitro and in vivo differentiation assays

References:

1. Crino, P.B., K.L. Nathanson, and E.P. Henske, *The tuberous sclerosis complex.* N.Engl.J.Med., 2006. **355**(13): p. 1345-1356.
2. Delaney SP, LM Julian, and WL Stanford, *The neural crest lineage as a driver of disease heterogeneity in Tuberous Sclerosis Complex and Lymphangioleiomyomatosis*. Frontiers in Cell & Developmental Biology, 2014 **2**:69, doi: 10.3389/fcell.2014.00069
3. Kristof, A.S., *mTOR Signaling in Lymphangioleiomyomatosis.* Lymphat.Res.Biol., 2010. **8**(1): p. 33-42.

4. Sarbassov, D.D., et al., *Prolonged Rapamycin Treatment Inhibits mTORC2 Assembly and Akt/PKB.* Mol.Cell, 2006. **22**: p. 159-168.
5. Bissler, J.J., et al., *Sirolimus for angiomyolipoma in tuberous sclerosis complex or lymphangioleiomyomatosis.* N Engl J Med, 2008. **358**: p. 140-151.
6. Davies, D.M., et al., *Sirolimus therapy in tuberous sclerosis or sporadic lymphangioleiomyomatosis.* N Engl J Med, 2008. **358**(2): p. 200-203.

KEYWORDS

Tuberous Sclerosis Complex (TSC)
Lymphangioleiomyomatosis (LAM)
induced pluripotent stem cells (iPSCs)
embryonic stem cells (ESCs)
reprogramming
CRISPR/Cas9 genome editing
neural stem cells (NSCs)
neural crest cells (NSCs)
models of human disease
cancer

ACCOMPLISHMENTS

We will describe our accomplishments in the second year of the study in relationship to our Statement of Work and the work we completed in year 1 and reported in last year's report. As detailed below, despite some technical challenges, we are on-track for completing the 3-year project on time. *Two manuscripts are currently being written based on this project*.

Aim 1: Generate TSC2 heterozygous and homozygous human iPSC and ESC lines.

We completed all of our Aim 1 tasks specified in our Statement of Work despite a mycoplasma infection that required us to re-derive a number of cell lines. Furthermore, as described in Task c below, we performed TSC2 genome editing with CRISPR/cas9 in two additional human pluripotent stem cell lines (WA07 (H7) – female cell line registry #0061; and a control male iPSC lines generated and validated in our lab, 168-1d2) to further ensure reproducibility of our results.

Major Task 1) Clone and validate inducible shRNA vectors (Expected time-line: 0-12 months).

This task was completed in the first year of the project and reported as Figure 1 in the 2014-2015 Progress Report, which is not included here.

Major Task 2-1) Generate TSC2 heterozygous and homozygous male (WA01, NIH Registration number: 0043) and female (WA09, NIH Registration number: 0062)) ESCs using CRISPR/Cas9 genome editing (Expected time-line: 0-12 months).

Last year we reported using CRISPR/Cas9 genome editing to generate TSC2 heterozygous and homozygous mutations in TSC2 in two NIH registered human ESC lines (male WA01 and female WA09). Two different mutations were engineered: 1- deletion of exon 3 to generate a null allele (**Figure 1**), and 2- an in-frame deletion of exon 11, mimicking a mutation reported in some patients with TSC-LAM (Fokkema et al., 2011; Au et al., 2007), leading to a near full-length protein that lacks the TSC1 binding domain (**Figure 2**). Our strategy is important because we can use these cell lines with the same engineered mutations to test why only women develop LAM. However, we discovered after the generation of these mutations that our targeted cell lines had been contaminated with mycoplasma. This required us to regenerate the CRISPR/cas9 genome edited cell lines. We are currently sub-cloning the WA01 (H1) *TSC2*$^{-/-}$ cell lines. Otherwise, all aspects of this task have been accomplished.

In remaking these cell lines, we added two additional human pluripotent stem cell lines to further ensure the reproducibility of our results (WA07 (H7) – female cell line registry #0061; and a control male iPSC lines generated and validated in our lab, 168-1d2). Therefore, any sex-specific differences in our cell lines would be confirmed not only by two clones (technical replicates) but two cell lines (biological replicates). Moreover, we added an additional feature in the TSC2 heterozygous and TSC2 homozygous deficient ESC lines. We have also introduced constitutive eGFP and TdTomato expression in the cell lines so that we can follow the mutant cells by monitoring the percentage of green or red cells in culture or in vivo. This allows us to directly assess the growth rates of wild type, TSC2 heterozygous and TSC2 homozygous deficient cells and test hypotheses that TSC2 heterozygous support the growth of TSC2 deficient cells (**Figure 3**). All cell lines are mycoplasma negative.

Major Task 2-2) Generate patient-derived TSC2 heterozygous and TSC2 deficient iPSC lines (Expected time-line: 7-15 months).

In addition to the cell lines generated in the first year and discussed in in the 2014-2015 Progress Report (TSC2-hypomorphic hESCs (**Figure 4A**), TSC2+/- patient-derived iPSCs (**Figure 4B**) and SMCs (**Figure 4C**)), we have generated TSC2 hypomorphic neural crest cell lines from iPSCs transduced with our inducible shRNA vectors (**Figure 4D**). These cell lines exhibit mTOR activation and expression of the LAM biomarker VEGF-D. We have also generated TSC2 hypomorphic fibroblast lines (**Figure 4E**), which we have used for iPSC reprogramming and induced neural stem cell (iNSC) experiments. We have focused our efforts on generating these additional cell lines because our preliminary data have strongly suggested that the neural crest lineage is a cell of origin for LAM and that TSC2 deficiency drives preferential differentiation into the neural and neural crest lineages (discussed further below). The additional cell lines now allow us to robustly test these hypotheses.

Major Task 3) Validate TSC2 heterozygous and homozygous iPSC and ESC lines using in vitro and in vivo (teratoma) assays (Expected time-line: 7-15 months).

We have performed a variety of in vitro and in vivo assays to validate the cell lines that we have generated. First of all, we performed karyotyping on all the cell lines we generated (some examples are shown in **Figure 5**). We have tested TSC2 deficient cells for pluripotency in vitro and in vivo, by marker gene and protein expression as well as the ability to generate cells of all three germ layers (**Figures 6-7**). We found that not all cell line clones have normal karyotypes and a few could not give rise to all three germ layers. However, at least 2 clones from each iPSC line and genome edited pluripotent stem cell line have normal karyotypes and are fully pluripotent. Only these validated cell lines are used in the experiments for this project and the modeling of TSC and LAM.

Interestingly, the TSC2 homozygous mutant female but not male cell lines generated by genome editing demonstrate profound cell fate alterations that support our hypothesis that neural crest cells are the LAM cell of origin (**Figure 8**). Unfortunately, the reviewers suggested that we *not* pursue in vivo modeling of LAM. Hence, we have not pursued this interesting and important data. We will look for other support to pursue in vivo modeling of LAM and TSC.

Milestone #1: *The establishment and validation of human TSC2 deficient primary cells* (Expected time-frame: 15 months).

With the exception of the WA01 (H1) *TSC2*$^{-/-}$ cell lines, all aspects of this Milestone have been met. In the next 3 months, the WA01 (H1) *TSC2*$^{-/-}$ cell lines will also be validated.

Aim 2: Model TSC and LAM using in vitro differentiation assays.

Major task 4: In vitro differentiation into candidate cells of origin of TSC tumors and model TSC and LAM *in vitro* (Expected time-line: 13-36 months).

Subtasks 1-2: Differentiation into neural stem cells (NSCs), neural crest cells NCCs and neural crest-derived smooth muscle cells (SMCs) (Expected time-line: 13-36 months).

Consistent with our analysis in vivo (**Figure 8**), we have determined that TSC2 deficiency promotes neural and neural crest differentiation. As shown in **Figure 9**, we have established protocols for NSC, NC and SMC differentiation from PSCs, and NSC induction from fibroblasts. NSCs and NCCs are generated from PSCs using a dual SMAD inhibition approach, with cell density at plating and the timed addition of a Wnt pathway agonist distinguishing NSC versus NCC differentiation. TSC2 deficient cells are more motile than wild type cells in vitro (**Figure 3**) and

potentially in vivo. For example, although the teratomas were formed by injecting the undifferentiated iPSCs and ESCs into the tibialis anterior muscle (leg muscle) in female immune deficient mice, we identified human TSC2 deficient cells in the kidney and lungs of a couple of animals but never from wild type iPSCs and ESCs.

SMCs are generated by addition of TGF-B to NCC cultures. We have also established a protocol for the isolation and growth of LAM-like patient-derived SMCs by culturing patient iPSC-derived teratoma explants under SMC growth conditions (**Figures 3, 9**). We have differentiated our TSC2 hypomorphic and CRISPR-Cas9 edited PSC lines into both the neural and NC lineages in vitro. We have observed enhanced expression of NSC and NC markers at early stages of differentiation (**Figure 9E**), as well as enhanced generation of SOX2 induced NSCs from TSC2-reduced fibroblasts (**Figure 9F**). With our TSC2 hypomorphic and deficient cell lines as well as robust NC and NSC protocols now in hand, we are undertaking experiments to quantitatively determine the effects of TSC2 loss on differentiation into the neural and neural crest lineages.

Subtask 3: Compare transcriptome and phosphoproteome of iPSC-derived cells and human TSC tumors (Expected time-line: 13-36 months).

We have not yet begun these experiments as it has been crucial to identify the best samples in which to perform these analyses. Thus, the sub-tasks 1-2, 4, and 7 are informing the experimental design of this subtask. We intend to start these experiments in the next 2-3 months, which will allow us to finish these experiments by the end of this 3-year project.

Subtask 4: Analysis of TSC2 mutant cell behavior (Expected time-line: 13-36 months).

Our hypothesis that neural crest-derived SMCs can model LAM is borne out by our cell behavior experiments. For example, **Figure 10** shows that TSC2 hypomorphic SMCs express a variety of LAM markers elevated P-S6K, HIF1a, VEGF-D, and GD3 as well as Estrogen Receptor alpha (ER-a). Furthermore, TSC2 hypomorphic cells demonstrate altered metabolic activity including reduced oxygen consumption and elevated levels of glycolysis based on Seahorse extracellular flux assays. Additional LAM/TSC cell behavior includes decreased levels of cellular autophagy and increased cell size. As summarized in **Figure 11**, TSC2 hypomorphic SMCs are a much better model of LAM than the only other TSC2 deficient human cell line (621-101 cells) that was established by immortalization of a LAM related renal tumor. *We are currently writing a manuscript describing the iPSC-derived TSC2 hypomorphic cell lines and their LAM-like cell behavior, which will be submitted in November 2016.*

To further model cell behavior of TSC/LAM cells generated from our TSC2 deficient human pluripotent stem cells, we have collaborated with the Shoichet Lab (University of Toronto) to study cell behavior in a lung-mimetic 3D hydrogel system. Their lab had previously developed stimuli-responsive, chemically-defined hydrogels that can be degraded by cell-secreted matrix metalloproteinases (MMPs) (Fisher et al., 2015), which are known to be secreted by LAM cells to enable their migration to other organs and causes the lung destruction associated with LAM. This is a better model to study cell invasion compared to other methods such as migration on a 2D surface, or using ill-defined scaffolds such as Matrigel and collagen. Designed to mimic the LAM native microenvironment, we have tuned the physical and chemical properties of these hydrogels to enable the selective MMP-mediated invasion of TSC mutant neural crest SMCs, which we have initially exploited with the iPSC-derived SMCs (**Figure 12A-C**). To quantify cell invasion at the end point of the experiment, we coat the top of these hydrogels with fluorescently-labeled microsphere beads (100 nm) and stain the cells cultured therein with fluorescently-labeled antibodies. Z-stack confocal images are acquired using a Cellomics high content imager, and the depth of cell invasion is measured using a novel algorithm we have developed. In brief, the XYZ co-ordinates of each cell is acquired, and subtracted from the gel surface, as detected by the fluorescent microspheres. We further confirm that cells are invading into these hydrogels via MMP-degradation by performing

zymography, **Figure 12D**. This is an entirely new strategy to model LAM. Interestingly, hypomorphic *TSC2*$^{+/-}$ SMCs expressed decreased levels of TSC2 when cultured on these 3D hydrogels compared to 2D culture, whereas wild type iPSC-derived SMCs expressed increased TSC2 expression **Figure 12F**, thus further supporting our hypothesis that cells cultured in these biomimetic 3D HA hydrogels better recapitulate their behaviors naturally found *in vivo*.

We reason that drugs will have different effects on target cells in tissue-mimetic 3D culture than 2D culture, with the 3D culture behavior being more reflective of in vivo effects. To test this hypothesis, we have begun testing a series of drugs associated with LAM. Although the clinical 'gold standard' is Rapamycin, this drug is tumoristatic and does not kill LAM cells, as evident by the decline of lung function in LAM patients following Rapamycin withdrawal. Our preliminary results show that performing drug screening using biomimetic 3D HA hydrogels provides additional readouts that are not possible using 2D polystyrene. While we do not observe any significant differences between 2D and 3D culture for cells treated with Rapamycin, Y-27632 (Rock inhibitor) and Simvastatin, we do observe that *TSC2*$^{+/-}$ SMCs are more chemosensitive to Saracatinib when cultured on 3D gels versus 2D (**Figure 13A**). In comparison to *TSC2*$^{+/+}$ (WT) SMCs, we do not observe selective cytotoxicity versus *TSC2*$^{+/-}$ cells (**Figure 13B**). Interestingly, Rapamycin does not prevent cell invasion by MMP-mediated mechanisms (**Figure 13C-D**), further showing the ineffectiveness of this clinically-used drug to prevent the tissue destruction elicited by MMPs. In contrast, Saracatinib and Simvastatin show decreased cell invasion, but the lack of specificity between the two cell types tested suggests that these drugs may not achieve selectivity to limit off-target side effects. Interestingly, Y-27632 (Rock inhibitor) is shown to decrease cell invasion of *TSC2*$^{+/-}$ SMCs while maintaining high cell viability of *TSC2*$^{+/+}$ (WT) cells.

A manuscript describing this work is currently in preparation and will be submitted within the next 4 months. We will continue optimizing hydrogel development by comparing wild type (WT) and TSC2-/- neural crest derived SMCs. We are continuing these experiments with our genome edited cell lines.

Subtask 5: Mitogen-activated signaling pathways and mTORC1 feedback inhibition of Akt signaling (Expected time-line: 13-36 months).

These experiments are underway. For example, **Figures 4D** and **10** report over-abundance of mTORC1 targets: P-S6, P-S6K, HIF1a, and Glut-1. We are continuing these experiments with our genome edited cell lines.

Subtask 6: mTORC1-dependent survival-related transcription factors (Expected time-line: 13-36 months).

These experiments are underway with our genome edited cell lines.

Subtask 7: Estrogen and prolactin signaling (Expected time-line: 13-36 months).

These experiments are underway. For example, we have observed estrogen receptor expression in the iPSC-derived *TSC2*$^{+/-}$ SMCs (**Figure 10D**).

Subtask 8: Unfolded protein (ER stress) response (Expected time-line: 13-36 months).

These experiments are underway with our genome edited cell lines.

References:

Au, K.S.*, et al.* Genotype/phenotype correlation in 325 individuals referred for a diagnosis of tuberous sclerosis complex in the United States. *Genetics in Medicine* **9**, 88-100 (2007).

Fokkema, I.F.*, et al.* LOVD v.2.0: the next generation in gene variant databases. *Human mutation* **32**, 557-563 (2011).

Fisher, S.A.*, et al.* Tuning the microenvironment: click-crosslinked hyaluronic acid based hydrogels provide a platform for studying breast cancer cell invasion. *Advanced Functional Materials* **25**, 7163-7172 (2015).

Figures

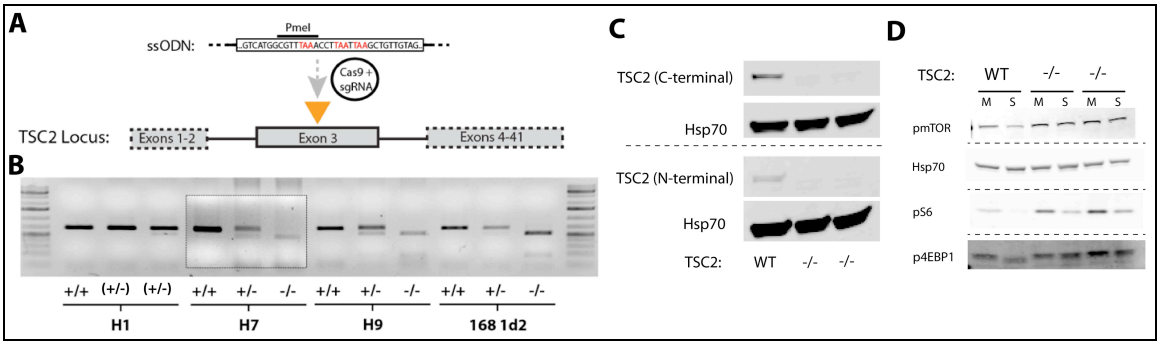

FIGURE 1. To generate a TSC2 null allele, exon 3 was targeted in H1, H7, H9, and 168-1d2 iPSCs. A) Through CRISPR/Cas9 mediated homologous recombination, a small termination sequence containing a unique restriction enzyme site was inserted into TSC2 exon3, resulting in a null allele. B) Digestion of TSC2 exon3 PCR amplicons using PmeI restriction enzyme reveals heterozygous and homozygous TSC2 null genotypes. H1 TSC2 null cell lines are currently undergoing subcloning to enrich for pure populations of edited clones. C) Homozygous insertion of the termination sequence results in undetectable levels of Tuberin expression, indicating full knockout of the TSC2 transcript. D) Increased levels of phosphorylated mTOR, S6, and 4EBP1 in TSC2 null cells grown in stress conditions (S) indicate constitutive mTOR activation as a result of loss of TSC2.

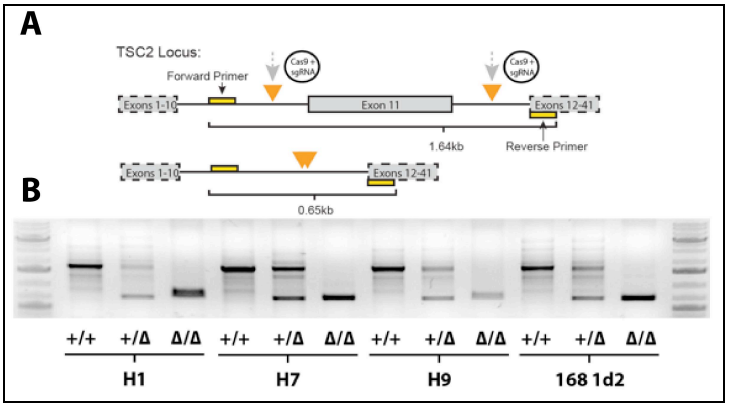

FIGURE 2: Generation of TSC2 ΔExon11 clones by genome editing in four differen human pluripotent stem cell lines. A) Schematic of the TSC2-Δ modification. B) TSC2-Δ genotypes of all four cell lines available for use in this project.

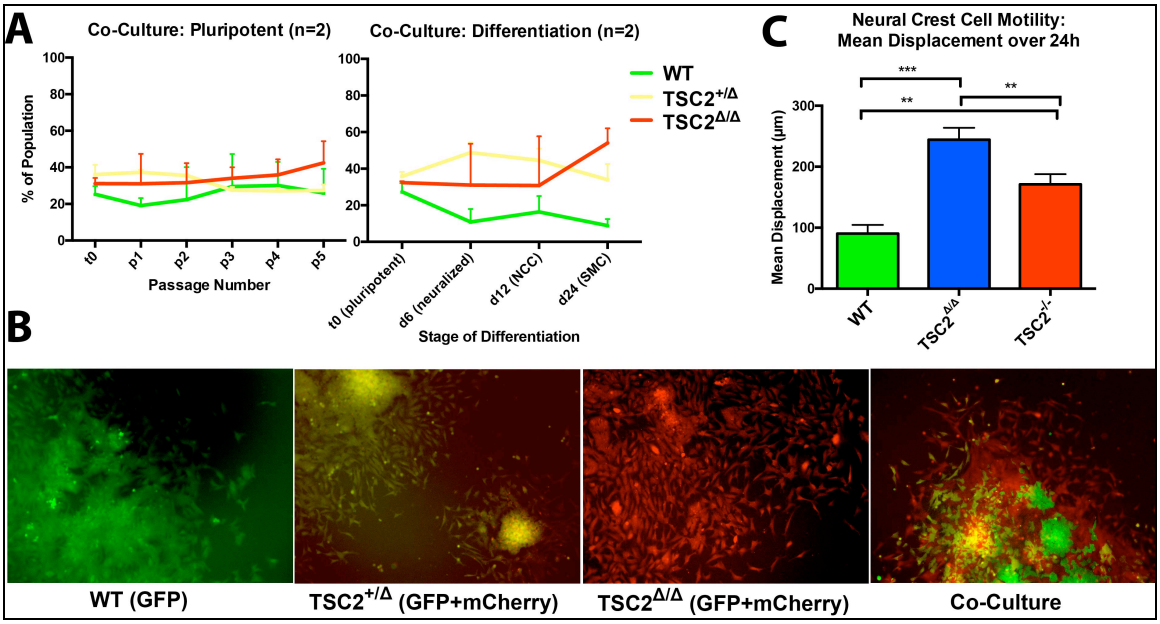

FIGURE 3: Fluorescent reporter tagging of the CRISPR/Cas9 TSC2 mutant cell lines used in this study allows us to investigate the influence of TSC2 genotype on cell behavior in co-cultures. A) Co-culture of WT, *TSC2*$^{+/\Delta}$, *TSC2*$^{\Delta/\Delta}$ H9 hESCs shows no evidence of genotype specific competitive growth over multiple passages. However, upon differentiation, a genotype-dependent growth advantage is observed. B) Genotype-specific fluorescent tagging effectively identifies genotypes in mixed co-cultures. Neural crest differentiation displays a genotype specific enhanced migratory phenotype of TSC2-Δ mutant neural crest cells from neuralized clusters. D) TSC2 mutant neural crest cells are significantly more motile than WT cells, with *TSC2*$^{\Delta/\Delta}$ displaying enhanced motility over *TSC2*$^{-/-}$ cells.

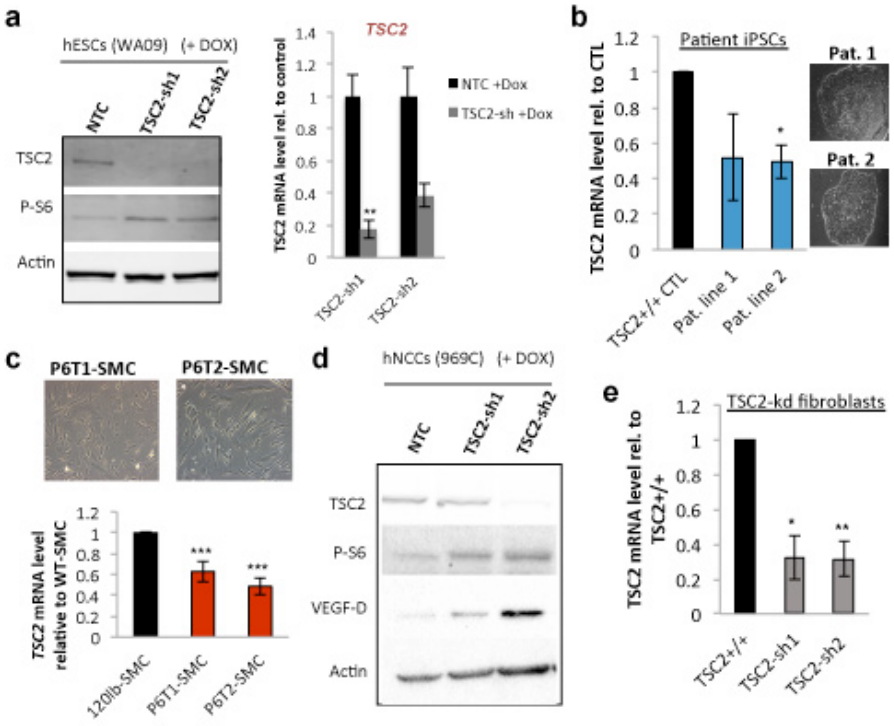

FIGURE 4. TSC2+/- and hypomorphic cell lines generated. (A) WA09 hESCs were transduced with Dox-inducible lentiviruses expressing non-template control (NTC) or two shRNAs directed against *TSC2* (TSC2-sh1, TSC2-sh2). Puromycin selected cells were cultured in the presence of 500ug/ml Dox for 1-3 weeks prior to harvest to induce shRNA expression. (A) Western blot analysis (left panel) demonstrates reduced expression of TSC2 and elevated phosphorylated-S6 protein (hyperactive mTOR) in TSC2-sh1 or sh2 cells compared to NTC. qRT-PCR analysis (A, right panel) demonstrates that *TSC2* levels are reduced to 18% and 39% of normal levels in TSC2-sh1 and TSC2-sh2 expressing cells, respectively. (B) qRT-PCR for *TSC2* in iPSC lines derived from an unaffected (TSC2+/+ CTL) individual or LAM patients (Pat. Line 1,2) shows half maximal levels of *TSC2* in patient-derived lines. (C) Control and patient-derived iPSCs were injected into immunocompromised mice for teratoma development, and tumour explants were cultured under smooth muscle cell (SMC) growth conditions. Cell morphology is shown and qRT-PCR for TSC2 in control (120lb-SMC) and patient-derived (P6T1/T2-SMC) SMC lines. (D) Human neural crest cells (hNCCs) were infected with NTC and TSC2-sh1/sh2 lentiviruses, selected and expanded in media containing 1ug/ml DOX. Western blot analysis shows reduced TSC2 expression correlates with mTOR activation (P-S6) and elevated VEGF-D expression. (E) qRT-PCR analysis of fibroblasts transduced with shRNA lentiviruses shows reduced TSC2 expression in TSC2-sh1/sh2 containing cells. *p<0.05, **p>0.01.

A

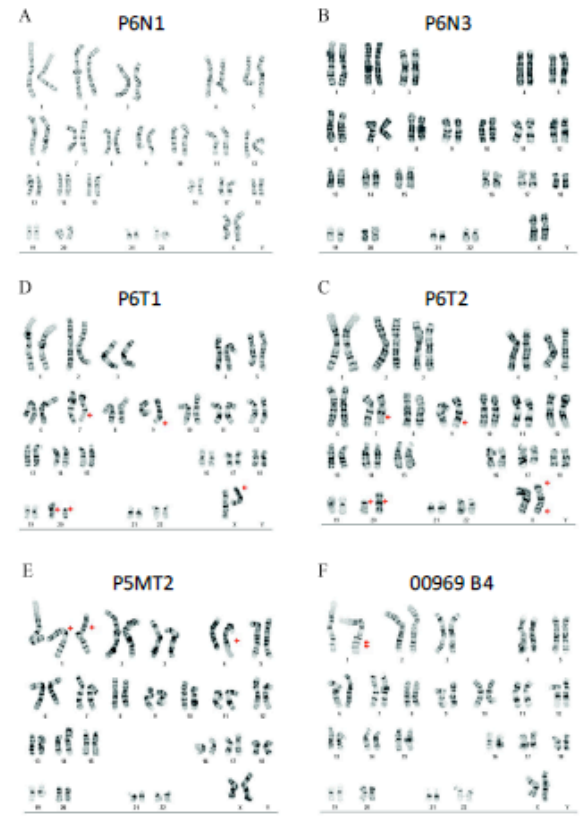

B

Sample	Karyotype
P6N1	46,XX
P6N2	46,X
P6N3	46,XX,i(20)(q10)[2]/46,XX[19]
P6T3	46,X,inv(X)(p22.1q28),t(7;20)(q22;q11.1),t(9;20)(q34;q11.2)[18]/ 47,X,inv(X)(p22.1q28),t(7;20)(q22;q11.1),t(9;20)(q34;q11.2),+15[cp2]
P6T1	46,X,inv(X)(p22.1q28),t(7;20)(q22;q11.1),t(9;20)(q34;p11.2)
P6T2	46,X,inv(X)(p22.1q28),t(7;20)(q22;q11.1),t(9;20)(q34;p11.2)
P6 R-noseB-k	46,X,inv(X)(p22.1q28),t(7;20)(q22;q11.1),t(9;20)(q34;p11.2)
P5N1	46,XX
P5N2	46,XX
P5N3	46,XX
P5MT1	46,XX
P5MT2	46,XX,t(1;4)(p22;q27)[14]/47,XX,+der(1)t(1;4)(p22;q27),t(1;4)(p22;q27)[6]
P5MT3	46,XX
P5FHT1	46,XX
P5FHT2	46,XX
P5FHT3	46,XX
00969 B4	46,XX,dup(1)(q32q42)
00969 B6	46,XX
00969 C1	46,XX

FIGURE 5. Karyotype analyses of iPSC lines and clones. iPSC lines and clonal derivatives of these lines were tested for genetic stability by karyotype analysis. Normal clones were identified for each patient; however, a much higher than normal abnormal karyotypes were detected compared to reprogramming other disease cells. In at least one case, the TSC tumor cells (P6 R-noseB-K) showed the chromosomal abnormality identified in the iPSC lines from this tumor (P6T1, 2, 3), demonstrating that this abnormality was present before reprogramming.

A

Sample	Pluripotency Markers			In vitro differentiation		
	ALP	SSEA-4	TRA-1-60	ectoderm	mesoderm	endoderm
P6N1	+	+	+	+	+	+
P6N2	+	+	+	+	+	+
P6T1	+	+	+	+	+	-
P6T2	+	+	+	+	+	-
P5N1	+	+	+	+	+	+
P5N2	+	+	+	+	+	+
P5N3	+	+	+	+	+	+
P5MT1	+	+	+	+	+	+
P5MT3	+	+	+	+	+	+
P5FHT1	+	+	+	+	+	+
P5FHT2	+	+	+	+	+	+
P5FHT3	+	+	+	+	+	+
00969 B6	+	+	+	+	+	+
00969 C1	+	+	+	+	+	+

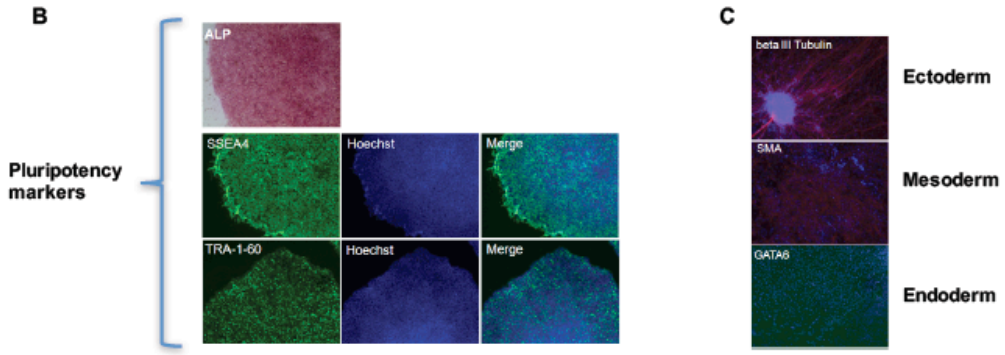

FIGURE 6. Normal pluripotency markers and in vitro differentiation for all clones used in this study. A-B. As an example of the in vitro validation experiments, all iPSC lines expressed pluripotent markers including alkaline phosphatase (ALP), SSEA4, and TRA-1-60. **C.** In vitro differentiation identified normal germ layer development for all but two clones with an abnormal karyotype derived from a TSC tumor with the same abnormal karyotype shown in Figure 5. Only fully pluripotent cells have been used in other experiments in this project.

A

Sample	Time to endpoint	Comments	Multipotent *in vivo* differentiation capacity
P6N1	10 weeks	Large leg tumors	+
P6N2	10 weeks	Large leg tumors	+
P6T1	11 weeks	Large leg tumors	+
P6T2	11 weeks	Large leg tumors	+
P5N1	11 weeks	Large leg tumors	
P5N2	10 weeks	Large leg tumors	+
P5N3	8 weeks	Large leg tumors	+
P5MT1	11 weeks	Large leg tumors	+
P5MT3	10 weeks	Large leg tumors	+
P5FHT1	8 weeks	Large leg tumors	+
P5FHT2	7 weeks	Large leg tumors	+
P5FHT3	9 weeks	Large leg tumors	+
00969 B6	10 weeks	Large leg tumors	+
00969 C1	8 weeks	Large leg tumors	+

B

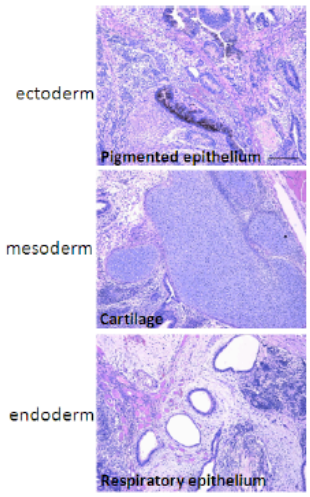

FIGURE 7. Normal teratoma formation by iPSCs used in this study. As shown in the Table (**A**), all but one iPSC line generated teratomas representing all three germ layers. **B.** Examples of normal in vivo differentiation are shown. Only fully pluripotent cells have been used in other experiments in this project.

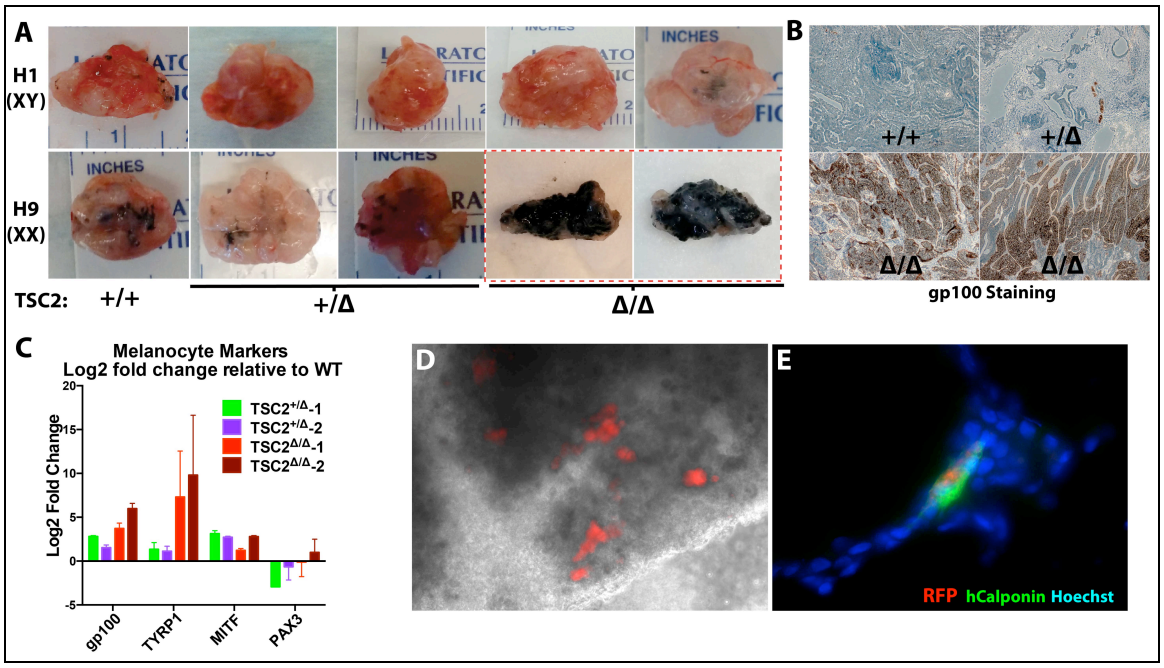

FIGURE 8. Female but not male TSC2 mutant cells differentiate in vivo into neural crest derived SMCs in female immunodeficient mice. A) Consistent with the female-associated pathology of LAM, only the tumors originating from female (H9) *TSC2*$^{\Delta/\Delta}$ hESCs resulted in highly pigmented teratomas. **B)** The pigmented tumors of the H9 TSC2$^{\Delta/\Delta}$ cells exhibit extensive staining for the LAM biomarker gp100, indicating that these tumors consist of melanin producing LAM-like cells. **C)** In TSC2 mutant teratomas, transcript levels of LAM/ melanocyte biomarker genes gp100, TYPR1, and MITF are all upregulated relative to *TSC2*$^{+/+}$ cells. Importantly, transcript levels of PAX3, a neural crest marker upregulated in metastatic melanoma, remain unchanged. This is indicates that the melanocyte-like cells generated in *TSC2*$^{\Delta/\Delta}$ teratomas are not melanoma cells. **D&E)** The *TSC2*$^{\Delta/\Delta}$ teratoma cells (tdTomato tagged) were taken into culture and were then injected into the lungs of NOD/scidIL2Rγ^{null} mice via intratracheal injection. The lungs were then excised after 2 months for analysis. Multiple small tdTomato^{+} tumors are clearly visible in lung tissue explants (**D**) indicating that the cells are able to enlodge and survive within the lungs. Immunohistochemical analysis of the lungs show that these small tdTomato^{+} express the smooth muscle marker, Calponin.

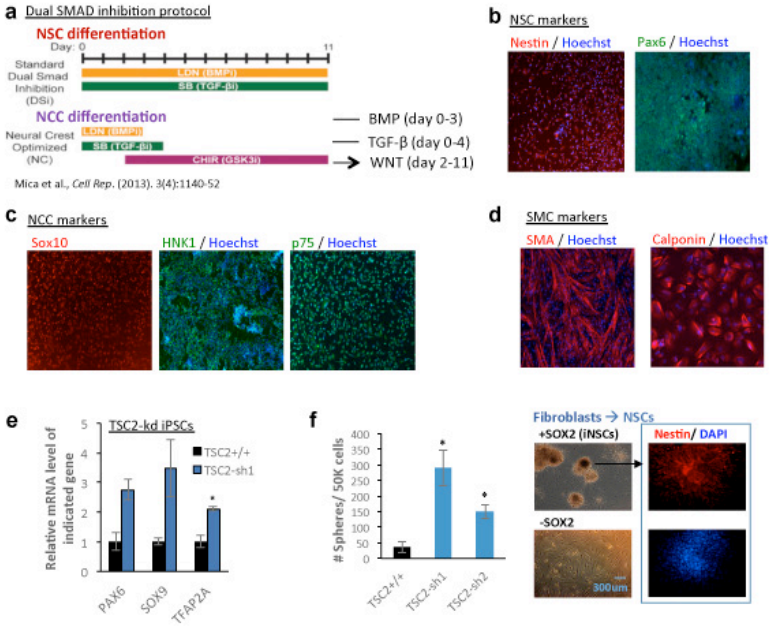

FIGURE 9. Differentiation into neural, neural crest and smooth muscle cell lineages, and preliminary data on effects of TSC2 deficiency on neural cell fate. (A) We have established a small molecule-based dual-SMAD inhibition protocol for the differentiation of human pluripotent stem cell cultures into neural stem cells (NSCs), based on timed inhibition of BMP and TGF-B signaling. Neural crest cells (NCCs) are generated with the additional activation of Wnt signaling using the small molecule CHIR (GSK3 inhibitor). Using these protocols we can generate cultures expressing classical NSC markers Nestin and Pax6 (B), and neural crest cultures expressing SOX10, HNK1 and p75 (C). (D) Treatment of NCC cultures for up to 2 weeks with TGF-B peptides induces wide-spread differentiation into the smooth muscle cell (SMC) lineage, marked by expression of smooth muscle actin (SMA) and Calponin. (E) Differentiating TSC2 reduced (TSC2-sh1) iPSCs exhibit increased expression of neural (Pax6, SOX9) and neural crest (SOX9, TFAP2A) markers compared to controls (TSC2+/+) at mid stages of differentiation. (F) Generation of induced NSCs (iNSCs) via SOX2 transduction and culture under NSC growth conditions is greatly enhanced from TSC2 reduced (TSC2-sh1/sh2) fibroblasts, as marked by an increased number of neurosphere-like clusters just 3-7 days post-transduction compared to a month for cells expressing normal levels of TSC2. *p<0.05.

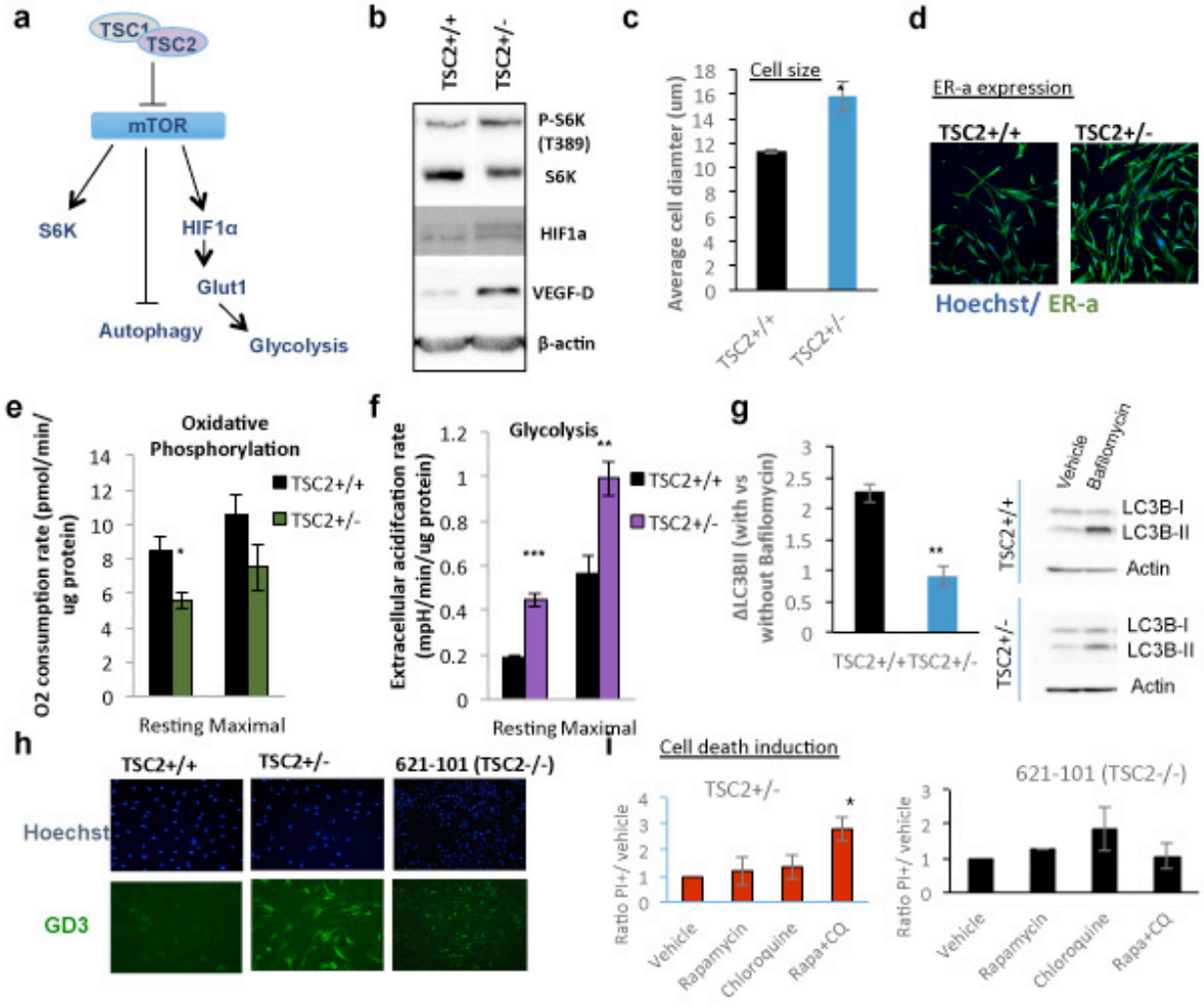

FIGURE 10. TSC2 hypomorphic patient-derived SMCs demonstrate LAM-like behavior. (A) Features of mTOR signaling examined in our assays. Note that many cell lines were analyzed but we show results from 1 control cell line (*TSC2*$^{+/+}$) and 1 patient-derived line (*TSC2*$^{+/-}$) as representative examples. (B) Western blot analyses demonstrate elevated P-S6K, HIF1a and VEGF-D in *TSC2*$^{+/-}$ SMCs (markers of mTOR signaling and LAM biomarkers). We also observe in *TSC2*$^{+/-}$ SMCs increased cell size (C), Estrogen Receptor alpha (ER-a) expression (D), reduced oxygen consumption (E) and elevated levels of glycolysis (F) based on Seahorse extracellular flux assays, decreased levels of cellular autophagy (G), and elevated expression of the LAM neural crest marker Ganglioside D3 (GD3) (H). Note GD3 expression is higher than in the *TSC2*$^{-/-}$ human LAM renal tumour-derived cell line 621-101. (I) Our *TSC2*$^{+/-}$ SMCs also show specific sensitivity to cell death (measured by propidium iodide staining via flow cytometry following 24 hour treatments) with combined treatment of the mTOR inhibitor Rapamycin and the autophagy inhibitor Chloroquine. *p<0.05, **p>0.01, ***p>0.001.

Cell line ID:	P6N1-SMC	P6N2-SMC	P6T1-SMC	P6T2-SMC	621-101
Reduced TSC2 expression	✓	✓	✓	✓	✓
SMC markers (SMA, Calponin)	✓	✓	✓	✓	✓
Elevated P-S6/ P-S6K	×	✓	✓	✓	✓
Elevated HIF1a	✓	✓	✓	✓	ND
Elevated VEGF-D	×	✓	✓	✓	×
Increased cell size	✓	✓	✓	✓	✓
Rapamycin responsiveness	✓	✓	✓	✓	✓
Glycolytic metabolism	✓	✓	✓	✓	ND
Reduced autophagy	✓	×	✓	✓	ND
Sensitivity to mTOR + autophagy inhibition	×	×	✓	✓	×
HMB45 expression	×	×	×	×	ND
GD3 expression	×	✓	✓	✓	×

FIGURE 11. Summary of iPSC-derived TSC2 hypomorphic SMCs lines compared to the only other human TSC2 deficient cells used to model LAM or other TSC mesenchymal neoplasms, 621-101 cells.

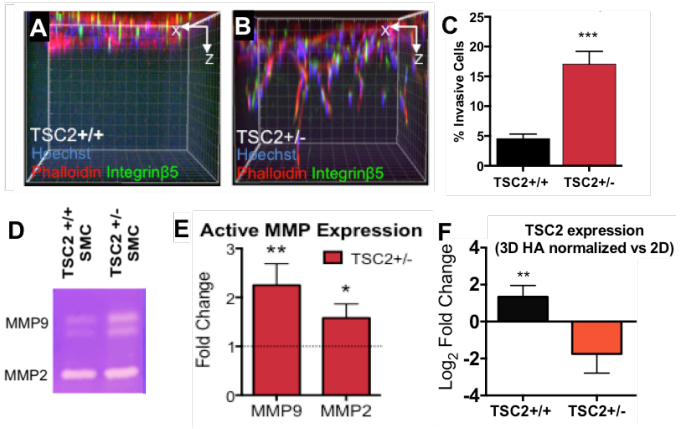

FIGURE 12. Stimuli-responsive 3D Hyaluronan (HA) hydrogels to model LAM cell behavior in a lung-mimetic 3D environment. iPSC-derived WT (*TSC2*$^{+/+}$) and *TSC2*$^{+/-}$ SMCs were used for these experiments. **A**,**B.** Z-stack confocal images and (**C**) quantification of *TSC2*$^{+/+}$ versus *TSC2*$^{+/-}$ cell invasion into 3D MMP-degradable gels (n=4). **D**. Zymography gel of *TSC2*$^{+/+}$ (WT) and *TSC2*$^{+/-}$ SMCs demonstrating that *TSC2*$^{+/-}$ SMCs produce more MMPs than WT cells. **E**. Quantification of MMP production of *TSC2*$^{+/-}$ SMCs expressed by fold change to WT SMCs (n=3). **F**. *TSC2*$^{+/-}$, but not *TSC2*$^{+/+}$ (WT), cells decrease TSC2 expression in 3D compared to 2D culture (n=3).

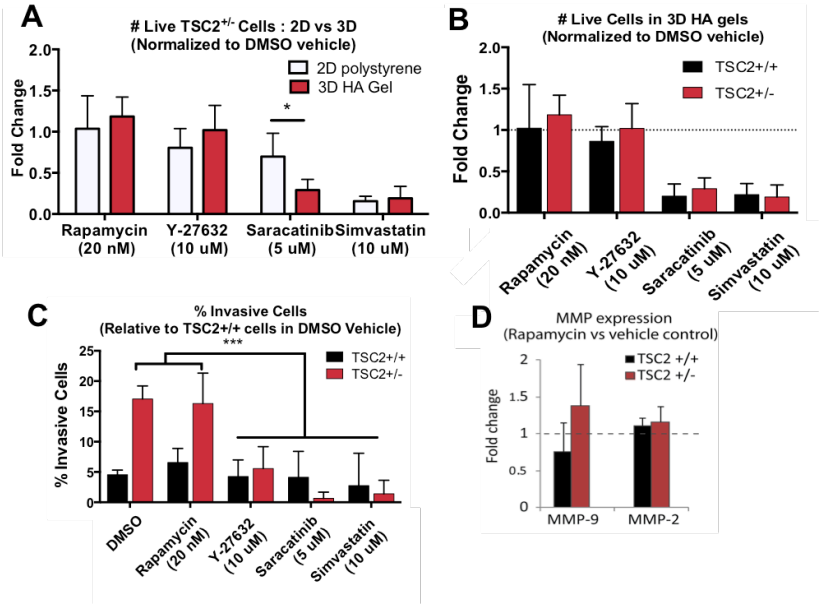

FIGURE 13. Drug screening using 3D biomimetic HA hydrogels provides differential and additional readouts not possible using 2D polystyrene. A. Drug response of *TSC2*$^{+/-}$ SMCs (WT) cultured on 2D polystyrene or 3D HA hydrogels. Treatment with 5 μM Saracatinib shows increased cell death in 3D vs on 2D, while no difference is observed with Rapamycin, Y-27632 (Rock inhibitor), or Simvastatin (n≥5). **B**. Drug response of *TSC2*$^{+/+}$ (WT) and TSC2$^{+/-}$ cells cultured on 3D HA hydrogels. Rapamycin and Y-27632 does not affect cell viability, while Saracatinib and Simvastatin increases cytotoxicity in both cell types (n≥5). **C.** *TSC2*$^{+/-}$ shows increased cell invasion relative to *TSC2*$^{+/+}$ SMCs when treated with DMSO. Treatment with Rapamycin (20 nM) shows no significant difference in cell invasion. Notably, *TSC2*$^{+/-}$ cells treated with Y-27632, Saracatinib, and Simvastatin all show decreased cell invasion versus DMSO controls (n=4). **D**. Treatment with Rapamycin does not prevent secretion of MMP2 or 9, thus supporting our data that Rapamycin does not prevent MMP-mediated cell invasion.

IMPACT

According to the journal, our article has been viewed and downloaded approximately 3000 times since it was published and referenced four times according to Google Scholar. For the limited size of the TSC and LAM field, this is a significant impact. Dr. Stanford was invited to give a lecture at the 2016 Rare Lung Disease Conference held in Cincinnati, Ohio. As a result, we have had several requests for our cell lines to labs in the USA, which have now been sent. Also, the two trainees supported by this grant, Sean Delaney and Dr. Lisa Julian, won two of the 5 total (best) poster awards at the 2016 Rare Lung Disease Conference.

We are currently writing two manuscripts based on the work supported by this application. The first is based on the iPSC-derived TSC2 hypomorphic cell lines and their LAM-like cell behavior. As summarized in **Figure 11**, these cells are a much better model of LAM than the only other TSC2 deficient human cell line (621-101 cells) that was established by immortalization of a LAM related renal tumor. The second manuscript is based on the development of the 3D lung-mimetic hydrogel to model LAM in vitro. In a year, we expect to have the data for at least one more manuscript, detailing our results from the TSC2 genome edited cell lines.

CHANGES/PROBLEMS

The project has progressed as expected; however, we ran into one major problem that we have overcome. The problem is that mycoplasma infected a number of human pluripotent stem cell lines in our lab. This included the stock line of WA09 (H9) and WA01 (H1) cells. We overcame this problem by implementing more frequent mycoplasma testing – now a minimum of every 3 months instead of yearly. Furthermore, we remade our gene targeted WA09 and WA01 cells. This slowed us down by about 6 months. Yet, we are still on target for our milestones since we remade cell lines in parallel with other work. While we were generating new targeted WA09 (H9) and WA01 (H1) cell lines, we also made targeted mutations in two other human pluripotent cell lines (WA07 (H7) – female cell line registry #0061; and a control male iPSC lines generated and validated in our lab, 168-1d2) to firmly establish that the phenotypes of the mutant cells are due to the induced mutations and sex of the cell lines and not the genetic makeup of those individual cell lines.

In addition, to better analyze the behavior of TSC2 deficient cells in vitro, we collaborated with Dr. Molly Shoichet at the University of Toronto to develop a lung-mimetic hydrogel to assess cell behavior in 3D, as in vivo. In fact, as shown in **Figures 12-13**, the lung-mimetic hydrogel elicited strong LAM phenotypes from TSC2 deficient cells.

PRODUCTS

We have published the following manuscript:

- Delaney SP, LM Julian, and WL Stanford. The neural crest lineage as a driver of disease heterogeneity in Tuberous Sclerosis Complex and Lymphangioleiomyomatosis. **Frontiers in Cell & Developmental Biology** November 25; 2:69 (p.1-15), 2014 doi: 10.3389/fcell.2014.00069

The following manuscript will be submitted for publication in the next few weeks:

- Julian LM[‖], SP Delaney[‖], Y Wang[‖], A Goldberg, RY Tam, C Doré, J Yockell-Lelièvre, G Giannikou, F McMurray, M-E Harper, EP Henske, DJ Kwiatkowski, TN Darling, J Moss, MS Shoichet, AS Kristof, and **WL Stanford**. Patient-derived *TSC2*-haploinsufficient smooth muscle cells exhibit widespread features of Lymphangioleiomyomatosis disease phenotypes. ([‖]equal contribution)

Dr. Stanford has given the following 7 lectures, which presented some of the material presented in this project report:

- "Pluripotent Stem Cells: from Modeling Disease to Therapeutics." University of Ottawa Health Symposium, Ottawa, ON, CANADA January 24, 2015
- "Pluripotent Stem Cells: from Modeling Disease to Therapeutics." Canadian Association of Research in Regenerative Medicine (CARRM), Ottawa, ON, CANADA March 7, 2015
- "Stem cell approaches to model human development and disease." The Annual Signal Transduction Research Group Symposium, University of Alberta, Edmonton, AB, CANADA May 11, 2015
- "Stem cell approaches to model human development and disease." Australian Regenerative Medicine Institute, Melbourne, Victoria, AUSTRALIA November 12, 2015
- "Stem cell approaches to model human development and disease." Murdoch Children's Hospital, University of Monash, Melbourne, Victoria, AUSTRALIA November 13, 2015
- "Stem cell approaches to model human development and disease." Beer Seminar Series, Meakins-Christie Laboratories/ McGill University Montreal, Quebec, CANADA February 8, 2016
- "A critical role for tissue mimetic cell culture and xenotransplantation in preclinical LAM models." 2016 Rare Lung Disease Conference/ LAM International Research Conference. The Francis G. Byrnes Platform Presentation Award. Cincinnati, OH USA September 23 – 25, 2016

The cell lines and lung tissue-mimetic hydrogel are being sent to collaborators in the USA and Canada.

PARTICIPANTS/ COLLABORATING INSTITUTIONS

Dr. William L Stanford
Site 1
University of Ottawa/OHRI
501 Smyth Rd.
Ottawa, ON Canada

Dr. Lisa Julian, postdoctoral fellow, Stanford lab, OHRI
Sean Delaney, doctoral student, Stanford lab, OHRI
Dr. Julien Yockell-Lelièvre, research associate, Stanford lab, OHRI
Carole Doré, technician, Stanford lab, OHRI

Dr. Arnold Kristof
Site 2
McGill University Health Centre
Royal Victoria Hospital
687 Pine Ave. W
Montreal, QC, Canada

Dr. Alexander Goldberg, postdoctoral fellow, Kristof lab, McGill University Health Centre

SPECIAL REPORTING REQUIREMENTS

NONE

APPENDIXES

None.